FIXED BED PYROLYSIS OF UNTREATED AND Ni (II) IMPREGNATED CORN GRAINS: EXPERIMENT AND MODELLING

Tănase DOBRE[1], Oana Cristina PÂRVULESCU[2], Laurențiu CEATRĂ[3], MARTA STROESCU[4], Anicuța STOICA[5]

S-a studiat piroliza boabelor de porumb netratate şi impregnate cu o soluție de azotat de nichel într-un reactor în strat fix, în atmosferă de dioxid de carbon. S-a obținut un reziduu solid, ulei pirolitic şi gaze necodensabile. Distribuția produşilor depinde de fluxul termic, viteza superficială a dioxidului de carbon şi concentrația soluției de nichel. S-a analizat influența acestor parametri asupra masei de reziduu solid, masei de ulei, duratei de operare, temperaturii stratului fix şi temperaturii peretelui reactorului. Pentru a descrie dinamica procesului s-a selectat un model cinetic global într-o singură etapă, ai cărui parametri au fost determinați din datele experimetale.

Slow pyrolysis of corn grains impregnated or not with a nickel nitrate solution was performed in a fixed bed reactor under carbon dioxide atmosphere. This produced a char, pyrolytic oil and incondensable gases. The distribution of these fractions was dependent on variations in heat flux, carbon dioxide superficial velocity and nickel solution concentration. The influence of these process variables on char mass, oil mass, operation time, material bed centre temperature and reactor wall temperature was studied. A one-stage global reaction kinetic model was selected to describe the process dynamics and its parameters were estimated based on experimental data.

Keywords: pyrolysis, corn, biomass, factorial experiment, kinetic model

1. Introduction

Vegetal materials are abundant, clean and cheap sources of renewable energy with a great potential to replace conventional fossil fuels. They can be

[1] Prof., Faculty of Applied Chemistry and Materials Science, University POLITEHNICA of Bucharest, Romania
[2] Eng., Faculty of Applied Chemistry and Materials Science, University POLITEHNICA of Bucharest, Romania, e-mail: oana.parvulescu@yahoo.com
[3] Eng., Faculty of Applied Chemistry and Materials Science, University POLITEHNICA of Bucharest, Romania,
[4] Eng., Faculty of Applied Chemistry and Materials Science, University POLITEHNICA of Bucharest, Romania,
[5] Prof., Faculty of Applied Chemistry and Materials Science, University POLITEHNICA of Bucharest, Romania,

converted into convenient solid, liquid and gaseous fuels by thermo-chemical and biological conversion technologies. The thermo-chemical processes, such as pyrolysis, gasification and combustion, lead to lower emissions of SO_2, NO_x and soot, due to negligible content of sulphur, nitrogen and ash of vegetal materials. Reduced amounts of CO_2 are achieved because a part of CO_2 released by conversion will be recycled into the plants by photosynthesis. Vegetal materials resources include wood and wood wastes, agricultural crops and their waste by-products, wastes from food processing, aquatic plants, algae etc. They contain polysaccharides (cellulose, hemicellulose, lignin, starch), monosaccharides, oligosaccharides, fats, proteins, ash, water and other compounds.

Vegetal materials pyrolysis, consisting of solid thermal degradation without oxygen, is usually performed in the presence of a carrier gas which can be inert (nitrogen, argon) or oxidant (carbon dioxide, steam). The pyrolysis products are lumped into three groups: permanent gases, a pyrolytic liquid (bio-oil/tar) and a solid residue (char), or simply into volatiles and char. These products result from both primary reactions of solid material devolatilization and secondary reactions of primary products degradation, i.e. cracking of condensable volatile organic compounds into low molecular weight gases and char aromatization, respectively [1-6].

Pyrolysis products distribution depends on heating rate, process temperature, operation time, type and flow rate of carrier gas, reactor type, raw material properties (chemical composition, size, shape, density, pretreatment) etc. An increase in volatiles production and a decrease in char amount with heating rate increasing were reported [6-8]. Referring to the process temperature influence, it is obvious that an increase in operation temperature produces a decrease in char yield as well as an enlargement of volatiles yield. At temperatures less than 500 ^{0}C, incondensable gases and oil production increases with temperature increasing, whereas at temperatures higher than 500 ^{0}C, gas yield increases and oil yield decreases with temperature increasing, as effect of an enhancement of oil vapour cracking [4,6-17]. In comparison to a stationary fixed bed reactor, a rotary reactor increases the incondensable gases output and decreases the oil production, respectively [6].

Raw material properties have important effects on the process dynamics. Accordingly, an increase in grain size determines temperature gradients in the particle, so the temperature at the centre is lower than that at the surface, resulting an increase in solid amount and a decrease in oil production [4,6,18]. At temperatures higher than 500 ^{0}C, smaller particles favour the oil vapour cracking reactions with an increase in incondensable gases production, because the volatiles residence time in the reactor is longer when smaller particles are used [6]. Generally, particles sizes less than 1.3 mm do not affect the pyrolysis products yield [9,18].A higher lignin content as well as a large ash amount

contribute to a higher char yield [6,15]. A previous drying of vegetal material can determine a decrease in pyrolytic oil production [19]. Chemical pretreatment of vegetal structure with various activating agents, i.e. zinc chloride, sodium carbonate, potassium carbonate, leads to a high oil yield, due to an enhancement of intramolecular dehydration reactions in the impregnated material [10,11,14]. An important production of hydrogen-rich pyrolytic gas can be obtained starting from a vegetal material impregnated with a nickel nitrate solution [1,5]. Some reactions occurring during the pyrolysis of nickel nitrate impregnated biomass are [5,20,21]:

(I) breaking of vegetal structure polymer chains producing char, hydrocarbons, carbon dioxide, water and carbon:

$C_nH_{2n}O_n \rightarrow C_{n-2}H_{2(n-2)}O_{n-2} + CH_4 + CO_2$

$C_nH_{2n}O_n \rightarrow C_{n-3}H_{2(n-3)}O_{n-3} + C_2H_4 + CO_2 + H_2O$

$C_nH_{2n}O_n \rightarrow C_{n-4}H_{2(n-4)}O_{n-4} + CH_4 + 2C + CO_2 + 2H_2O$

$C_nH_{2n}O_n \rightarrow$ char + hydrocarbons (C_mH_k) + $CO_2 + H_2O$

(II) reforming of generated hydrocarbons leading to syngas:

$CH_4 + CO_2 \rightarrow 2CO + 2H_2$

$CH_4 + H_2O \rightarrow CO + 3H_2$

$C_2H_4 + 2CO_2 \rightarrow 4CO + 2H_2$

$C_2H_4 + 2H_2O \rightarrow 2CO + 4H_2$

$C_mH_k + mCO_2 \rightarrow 2mCO + (k/2)H_2$

$C_mH_k + mH_2O \rightarrow mCO + (m+k/2)H_2$

(III) cracking of support and hydrocarbons:

$C_nH_{2n}O_n \rightarrow nC + nH_2O$

$CH_4 \rightarrow C + 2H_2$

$C_2H_4 \rightarrow 2C + 2H_2$

$C_mH_k \rightarrow mC + (k/2)H_2$

(IV) oxidation of C^0 to C^{+2}:

$C + CO_2 \rightarrow 2CO$

$C + H_2O \rightarrow CO + H_2$

(V) decomposition of nickel nitrate impregnated into porous structure in nickel oxide, nitrogen dioxide and oxygen::

$Ni(NO_3)_2 \rightarrow NiO + 2NO_2 + 1/2O_2$

(VI) reduction of Ni^{+2} to Ni^0:

$NiO + H_2 \rightarrow Ni + H_2O$

$NiO + CO \rightarrow Ni + CO_2$

$NiO + C \rightarrow Ni + CO$

(VII) consumption of nitrogen dioxide:

$2NO_2 + 4CO \rightarrow N_2 + 4CO_2$

$2NO_2 + 4H_2 \rightarrow N_2 + 4H_2O$.

$2NO_2 + 2\ C \rightarrow N_2 + 2CO_2$

During pyrolysis, metallic nickel (Ni^0) nanocrystallites are formed into porous vegetal structure, as demonstrated by X-ray diffraction (XRD), X-ray photoelectron spectroscopy (XPS), transmission electron microscopy (TEM) and temperature-programmed pyrolysis experiments [5]. These Ni^0 nanocrystallites act as a catalyst and activate some of the pyrolytic reactions, e.g. reforming, cracking and nitrogen dioxide consumption.

The pyrolytic gas and bio-oil can be employed as combustibles or raw materials sources, whereas the char is useful as a renewable fuel, activated carbon or carbon-supported catalyst. The paper focuses on the qualitative and quantitative characterization of fixed bed pyrolysis of corn grains impregnated or not with a nickel nitrate solution, in the presence of a carbon dioxide stream.

2. Experimental part

2.1. Materials

Untreated and Ni (II) impregnated corn grains were employed as vegetal material. The metallic salt used for the grains impregnation was $[Ni(NO_3)_2 \cdot 6H_2O]$. Whole corn grains with an equivalent spherical diameter of 8 mm were stirred with a nickel nitrate aqueous solution at a concentration of 300 g/L. Batch impregnation was performed for 72 hours at a solid-liquid ratio of 1:5. The corn grains were then filtered and dried in an oven at 105 ^{0}C for 72 hours. The mean percentage composition of a corn grain is listed in Table 1 [22].

Table 1

Composition of a corn grain

Compound	Starch	Proteins	Fibers	Fats	Sugars	Ash	Water
% wt.	62.7	8.2	8.2	3.7	2.2	1.2	13.8

The cross section of a corn grain shown in Fig. 1 reveals its main parts, i.e. hull, tip cap, germ and endosperm. The hull and tip cap, accounting for about 6-8% of the grain weight, have a high content of fibers (≈90%). The germ (embryo), containing a high amount of fats, is about 10-12%. The remainder of the grain is endosperm which consists of 85-90% starch, 8-10% proteins (gluten) and a small amount of fats and other compounds [23]. In endosperm, the starch granules are encased in a continuous proteins matrix. Characteristic gluten matrix of horny endosperm is very dense and the starch particles are held more firmly, whereas in floury endosperm the matrix is less dense and starch granules are dispersed loosely. Accordingly, the starch granules in floury endosperm can be thermal degraded easier than in horny endosperm.

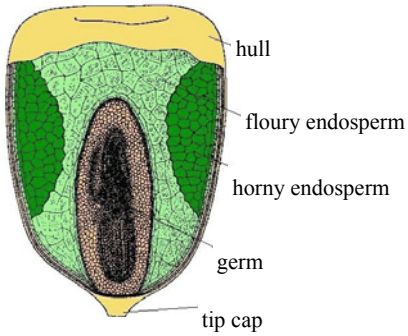

Fig. 1. Structure of a corn grain [23].

2.2. Equipment and procedure

The laboratory set-up used for pyrolysis process study was described in our previous studies [20,21,24]. A 400 g sample of vegetal material is introduced in a 50 mm diameter and 500 mm height quartz column. The column wall is heated by an electric resistance with a preset heat flow. The carbon dioxide from a cylinder, whose flow is measured by a flow-meter and controlled by a pressure reducer, is fed into the column by a pipe, up-flows through the material fixed bed and is evacuated with the volatiles obtained during the pyrolysis. The mixture of gases and vapours is cooled in a condenser, producing pyrolytic oil and incondensable gases. Vegetal material mass, oil mass, column wall temperature and bed centre temperature are recorded and collected by a data acquisition system.

The final char obtained by impregnated material pyrolysis was analysed by means of a Bruker-AXS D8 ADVANCE X-ray diffractometer, using Cu Kα radiation operating voltage of 40 kV and current of 40 mA. Nickel crystallite size was calculated by Scherrer formula:

$$d = \frac{K\lambda}{\delta \cos\theta} \tag{1}$$

where d is the equivalent spherical diameter of crystallite, K the shape factor (K=0.9), λ the X-ray wavelength (λ=0.154 nm), δ the peak width at half peak height and θ the diffraction angle ($10^o \leq \theta \leq 55^o$).

2.3. Experimental variables

Pyrolysis experimental study was conducted at two values (levels) of process independent variables (factors), i.e. heat flux, q, carbon dioxide superficial velocity, w, and nickel nitrate solution concentration, c. A set of 8 experiences was carried out according to a 2^3 factorial plan (Table 2).

Table 2

Process factors levels

Exp.	q (W/m^2)	w (m/h)	c (g/L)
1	2600	1	0
2	2600	2	0
3	3470	1	0
4	3470	2	0
5	2600	1	300
6	2600	2	300
7	3470	1	300
8	3470	2	300

Vegetal material mass, m, oil mass, m_{oil}, bed centre temperature, t_c, and column wall temperature, t_w, were continuously recorded as a function of heating time, τ. Each experience was replicated three times to determine its reproducibility, which was found to be good.

3. Results and discussion

3.1. Pyrolysis experimental curves

Time variation curves of vegetal material mass, m/m_0, and oil mass, m_{oil}/m_0, given in Fig. 2, have the same shape of bent step. A decrease in char yield and an enlargement of oil production occur at a high value of heat flux and in case of impregnated material.

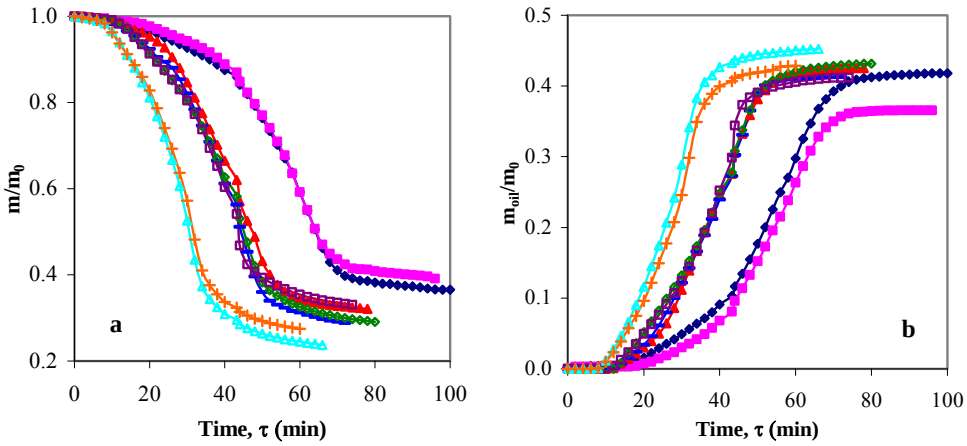

Fig. 2. Time variation of: a) vegetal material mass; b) oil mass
(♦ exp 1, ■ exp 2, ▲ exp 3, – exp 4, ◊ exp 5, □ exp 6, △ exp 7, + exp 8).

Temperature dynamics of material bed centre, t_c, and column wall, t_w, shown in Fig. 3, prove that the temperatures increase with heat flux increasing. The impregnation produces a sharp increase of t_c and a slight increase of t_w until 250-350 ^{0}C, followed by a constant plateau, which is probably due to the endothermic reactions of catalytic reforming and cracking. Characteristic curves of mass and temperature dynamics in Figs. 2 and 3 highlight that the pyrolysis is more rapid at high levels of all process factors.

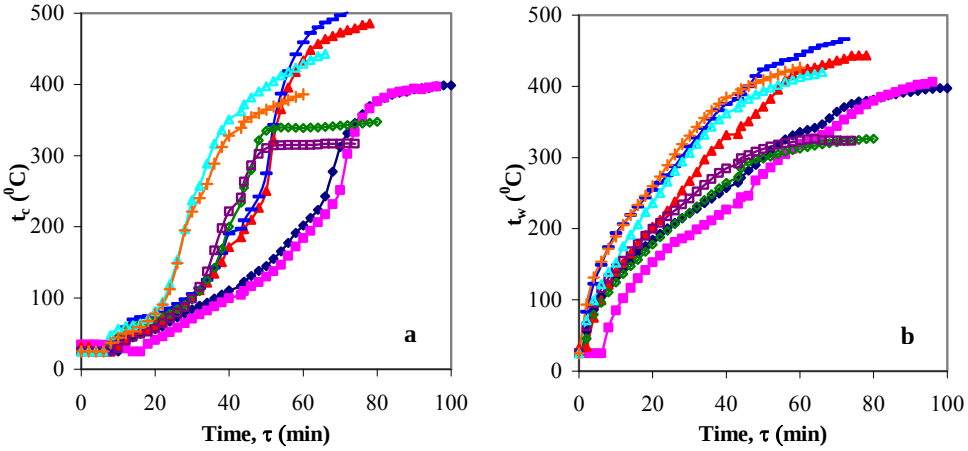

Fig. 3. Time variation of: a) bed centre temperature; b) wall temperature (♦ exp 1, ■ exp 2, ▲ exp 3, – exp 4, ◊ exp 5, □ exp 6, △ exp 7, + exp 8).

Fig. 4 shows material mass loss rate, $-d(m/m_0)/d\tau$, depending on logarithmic mean temperature between bed centre and column wall, t_m. A slight mass loss from ambient temperature to about 130 ^{0}C occurs due to material moisture removal.

Each differential curve in Fig. 4a has two relevant peaks, emphasizing that the pyrolysis of untreated material develops intensely in two main stages. The first stage, characterized by smaller peak amplitudes (0.013-0.027 min^{-1}) and peak temperatures $(t_m)_{peak}$=186-272 ^{0}C, can be attributed to the starch degradation in floury endosperm, whereas the second stage, with higher peak amplitudes (0.022-0.029 min^{-1}) and $(t_m)_{peak}$=245-307 ^{0}C, can be an effect of the starch degradation in horny endosperm.

Each differential curve in Fig. 4b has a single relevant peak, emphasizing that the pyrolysis of impregnated material develops intensely in a main stage. This stage is characterized by peak amplitudes ranging between 0.028 min^{-1} and 0.045 min^{-1} and peak temperatures $(t_m)_{peakc}$=281-288 ^{0}C. Accordingly, in contrast with

the characteristic differential curves of untreated grains pyrolysis (Fig. 4a), which have two relevant peaks, the curves $-d(m/m_0)/d\tau=f(t_m)$ in Fig. 4b have a single relevant peak. This is in compliance with data reported in the related literature, i.e. an increase in biomass impregnation degree reduces the distance between the peaks and the peaks overlap at a certain value of impregnation degree [25].

The values of maximum material loss rate, $[-d(m/m_0)/d\tau]_{peak}$, and of corresponding logarithmic mean temperature, $(t_m)_{peak}$, under various operation conditions, are summarized in Table 3. Tabulated data show that the peak height and the corresponding temperature are greater at high value of heat flux, in compliance with the data reported in the related literature [18,26-30].

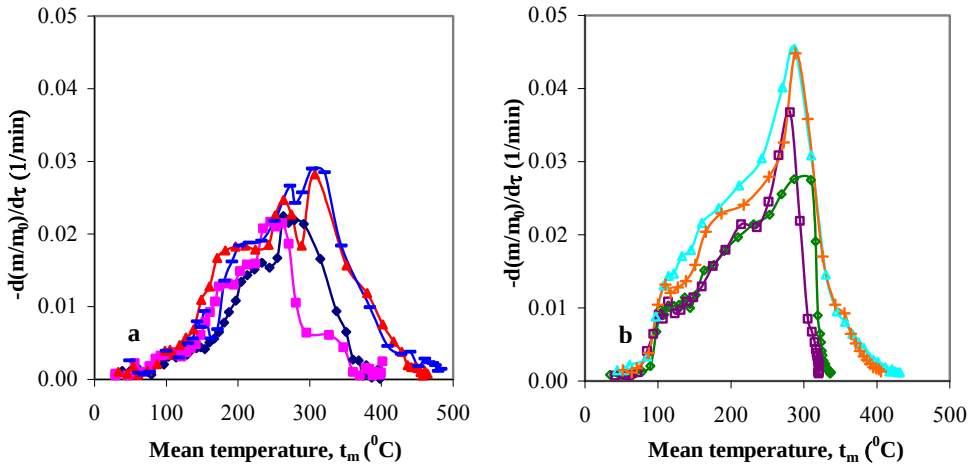

Fig. 4. Mass loss rate versus logarithmic mean temperature for: a) untreated material; b) impregated material (♦ exp 1, ■ exp 2, ▲ exp 3, – exp 4, ◊ exp 5, □ exp 6, △ exp 7, + exp 8).

Table 3

Maximum material loss rate and corresponding peak temperature

Exp.	$[-d(m/m_0)/d\tau]_{peak}$ (1/min)		$(t_m)_{peak}$ (^{0}C)	
	1st stage	2nd stage	1st stage	2nd stage
1	0.016	0.022	233	271
2	0.013	0.022	186	245
3	0.025	0.028	264	307
4	0.027	0.029	272	304
5	0.028		287	
6	0.037		281	
7	0.045		287	
8	0.045		288	

3.2. Factorial experiment

Vegetal material mass, m, oil mass, m_{oil}, operation time, τ, material bed centre temperature, t_c, and column wall temperature, t_w, were selected as process dependent variables (responses). These variables can be linked to the process factors by adequate equations. Factors dimensionless values were calculated depending on natural values with the following correlations:

$$x_1 = \frac{q - 3035}{435} \tag{2}$$

$$x_2 = \frac{w - 1.5}{0.5} \tag{3}$$

$$x_3 = \frac{c - 150}{150} \tag{4}$$

Factors dimensionless values as well as responses final values divided by the initial material mass, i.e. $y_1 = \frac{m_f}{m_0}$, $y_2 = \frac{m_{oilf}}{m_0}$, $y_3 = \frac{\tau_f}{m_0}$, $y_4 = \frac{t_{cf}}{m_0}$ and $y_5 = \frac{t_{wf}}{m_0}$ are given in Table 4.

Table 4

Experimentation matrix

Exp.	q (W/m^2)	w (m/h)	c (g/L)	x_1	x_2	x_3	y_1	y_2	y_3 (min/g)	y_4 (^{0}C/g)	y_5 (^{0}C/g)
1	2600	1	0	-1	-1	-1	0.365	0.418	0.261	1.040	1.037
2	2600	2	0	-1	1	-1	0.391	0.366	0.251	1.036	1.060
3	3470	1	0	1	-1	-1	0.321	0.425	0.204	1.268	1.158
4	3470	2	0	1	1	-1	0.288	0.413	0.188	1.309	1.218
5	2600	1	300	-1	-1	1	0.290	0.432	0.235	1.021	0.959
6	2600	2	300	-1	1	1	0.331	0.412	0.217	0.931	0.951
7	3470	1	300	1	-1	1	0.237	0.452	0.194	1.303	1.236
8	3470	2	300	1	1	1	0.275	0.429	0.176	1.134	1.253

Processing the data listed in Table 4 based on the procedure recommended for a factorial experiment with 2 levels [31], the following correlations were obtained:

$$y_1 = 0.312 - 0.032x_1 + 0.009x_2 - 0.029x_3 - 0.008x_1x_2 + 0.005x_1x_3 + 0.011x_2x_3 + 0.007x_1x_2x_3 \tag{5}$$

$$y_2 = 0.418 + 0.011x_1 - 0.013x_2 + 0.013x_3 + 0.005x_1x_2 - 0.002x_1x_3 + 0.003x_2x_3 - 0.005x_1x_2x_3 \tag{6}$$

$$y_3 = 0.216 - 0.025x_1 - 0.008x_2 - 0.010x_3 - 0.001x_1x_2 + 0.005x_1x_3 - 0.001x_2x_3 + 0.001x_1x_2x_3 \tag{7}$$

$$y_4 = 1.130 + 0.123x_1 - 0.028x_2 - 0.033x_3 - 0.004x_1x_2 - 0.002x_1x_3 - 0.037x_2x_3 - 0.016x_1x_2x_3 \quad (8)$$

$$y_5 = 1.109 + 0.107x_1 + 0.012x_2 - 0.009x_3 + 0.008x_1x_2 + 0.037x_1x_3 - 0.009x_2x_3 - 0.002x_1x_2x_3 \quad (9)$$

Correlations (5)-(9), results listed in Table 4 and experimental data in Figs. 2 and 3 emphasize that:

- final values of solid mass, y_1, are low at superior levels of heat flux, x_1, and nickel nitrate solution concentration, x_3;
- final values of oil mass, y_2, are high at superior levels of x_1 and x_3 and inferior level of gas superficial velocity, x_2;
- minimum final values of operation time, y_3, are achieved at superior levels of all process factors;
- final values of bed centre temperature, y_4, and column wall temperature, y_5, are maximum at superior level of x_1.

3.3. Kinetic model

A one-stage global reaction model was adopted to describe the conversion process from raw material to char and volatiles [2,3,8,26-28,32]. For dynamic data obtained at a constant heating rate, $\beta = \frac{dT_m}{d\tau}$, the decomposition rate can be described by equation [32]:

$$\frac{d\alpha}{d\tau} = (1-\alpha)\frac{A}{\beta}\exp(-\frac{E}{RT_m}) \quad (10)$$

where volatiles conversion is expressed as:

$$\alpha = \frac{m_0 - m}{m_0 - m_f} \quad (11)$$

Taking natural logarithms on both sides of eq. (10) yields:

$$\ln\left(\frac{1}{1-\alpha}\frac{d\alpha}{d\tau}\right) = \ln\frac{A}{\beta} - \frac{E}{RT_m} \quad (12)$$

The values of pre-exponential factor, A/β, and activation energy, E, depending on operation conditions were obtained from the intercept and the slope of the straight line given by a plot of $ln\left(\frac{1}{1-\alpha}\frac{d\alpha}{d\tau}\right)$ versus $\frac{1}{T_m}$.

Characteristic values of kinetic parameters A/β and E, which were regressed based on experimental data under various operation conditions, are summarized in Table 5. Table 5 contains also the mean values of heating rate, β, as well as the ranges of temperature, t_m, and conversion, α, wherein the mean values of β were estimated. As can be seen, the pre-exponential factor and activation energy increase with heat flux decreasing.

Table 5

Effect of process factors on kinetic parameters

Exp.	Decomposition stage	$\beta=dT_m/d\tau$ (K/min)	t_m (^{0}C)	α	A/β (1/min)	E (kJ/mol)
1	1st	4.71	197-244	0.29-0.52	73	30.96
	2nd	4.78	255-292	0.57-0.85	1095	82.97
2	1st	3.61	121-194	0.10-0.38	1879	41.70
	2nd	4.77	203-271	0.43-0.87	4705	55.65
3	1st	6.62	183-275	0.28-0.70	13	22.71
	2nd	10.93	289-351	0.75-0.88	26	24.55
4	1st	7.75	216-280	0.36-0.61	43	28.56
	2nd	8.04	290-344	0.69-0.90	1431	43.47
5	1st	8.8	163-316	0.32-0.87	42	26.62
6		8.1	160-295	0.29-0.86	267	33.64
7		10.5	133-310	0.20-0.82	28	23.76
8		11.0	166-305	0.29-0.81	57	27.26

Fig. 5 compares the differential conversion curves predicted by estimated kinetic parameters with the experimental results. A good agreement between experimental and simulated data is proved (errors less than 10 %).

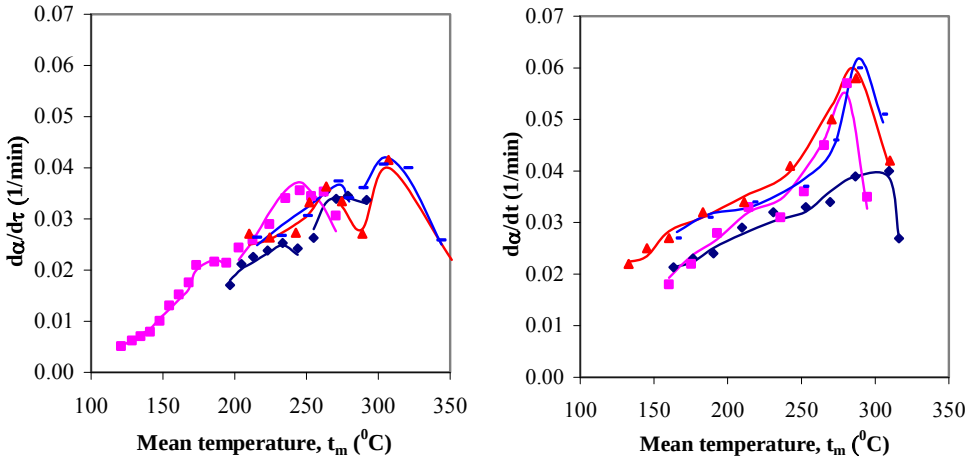

Fig. 5. Comparison between experimental (symbols) and simulated (lines) differential conversion curves (♦ exp 1, ■ exp 2, ▲ exp 3, – exp 4, ◊ exp 5, □ exp 6, Δ exp 7, + exp 8).

3.4. Characterization of nickel crystallites

Char XRD patterns in Fig. 6 emphasize two relevant peaks, appearing at about 44º and 52º, which are attributed to the presence of metallic nickel. Table 6 contains values of equivalent spherical diameter of nickel nanocrystallite, which were estimated by Scherrer formula for the highest peak, i.e. that obtained at 44º. As can be seen, the nickel nanocrystallite size increases with heat flux and carbon dioxide superficial velocity decreasing.

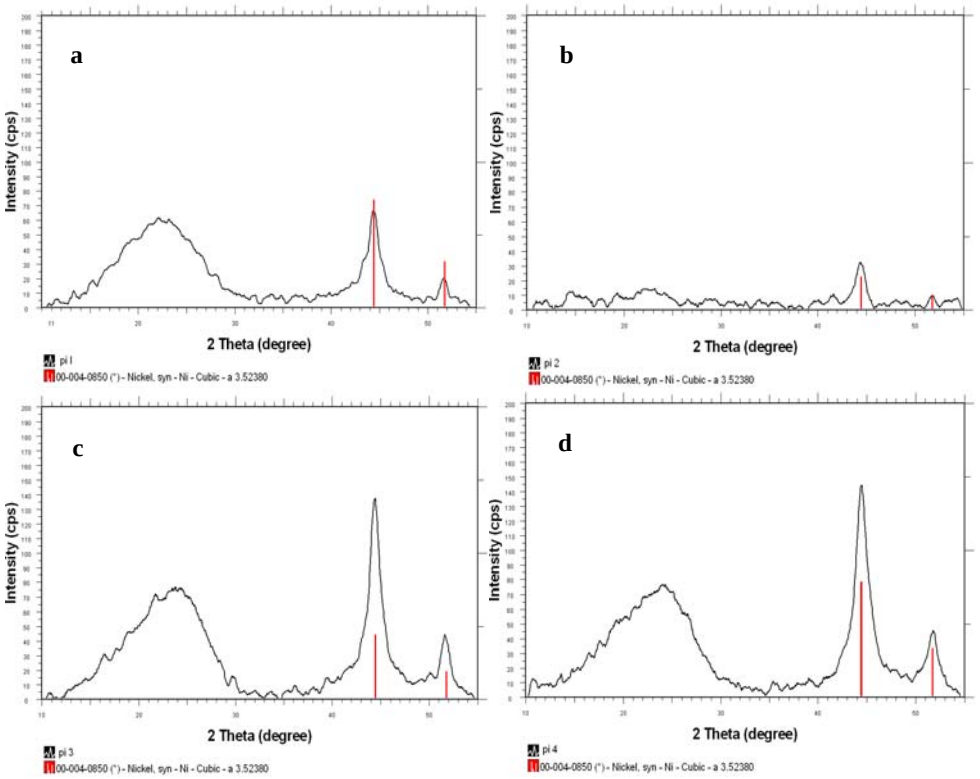

Fig. 6. XRD patterns of impregnated char: a) pi 1; b) pi 2; c) pi 3; c) pi 4.

Table 6

Nickel nanocrystallite size into impregnated char

Exp.	Final char code	*d* (nm)
5	pi 1	7.92
6	pi 2	7.54
7	pi 3	7.51
8	pi 4	6.04

4. Conclusions

An experimental set-up was designed and scaled-up in order to study the fixed bed pyrolysis of corn grains. Slow pyrolysis of corn grains impregnated or not with a nickel nitrate aqueous solution was conducted. Carbon dioxide was employed as a carrier agent and a reactant in the pyrolysis process. A char, a pyrolytic oil and a gaseous fraction were produced. During pyrolysis, metallic nickel nanocrystallites were formed into impregnated vegetal structure, as demonstrated by XRD experiments. The impregnated char will be used as a precursor of carbon-supported catalyst which will be tested in subsequent hydrogenation processes.

A process analysis by 2^3 factorial programming was performed, with the factors being heat flux, carbon dioxide superficial velocity and nickel nitrate solution concentration. Correlations between these factors and process dependent variables, namely char mass, pyrolytic oil mass, operation time, char bed temperature and column wall temperature were established for untreated and impregnated grains.

Under the study conditions, the heat flux and material impregnation had a significant effect on the process performances. A one-stage global reaction kinetic model, whose parameters were estimated based on experimental data, was selected to simulate the process dynamics. The model predicted well the real conditions and it could facilitate the design, scaling-up and operation of fixed bed pyrolysis reactors.

Acknowledgements

This work was supported by POSDRU ID project nr. 5159/2008.

Nomenclature

A/β	pre-exponential factor, 1/min
c	nickel nitrate solution concentration, g/L
d	equivalent spherical diameter of nickel crystallite, nm
E	activation energy, kJ/mol
K	shape factor
m	vegetal material mass, g
m_{oil}	pyrolytic oil mass, g
m_0	imitial vegetal material mass, g
q	heat flux, W/m^2
R	gas universal constant, R=8.314 J/mol K
t	temperature, ^{0}C
T	absolute temperature, K

w carbon dioxide superficial velocity, m/h
x_i process dimensionless factor, i=1…3
y_j process final response, j=1…5

Greek letters

α volatiles conversion
β heating rate, $\beta = \frac{dT_m}{d\tau}$, K/min
δ peak width at half peak height, nm
λ X-ray wavelength, nm
θ diffraction angle, º
τ time, min

Subscripts

c material bed centre
f final
m logarithmic mean
w column wall
0 initial

REFERENCES

[1] *K. Bru, J. Blin, A. Julbe and G. Volle*, "Pyrolysis of metal impregnated biomass: An innovative catalytic way to produce gas fuel", J. Anal. Appl. Pyrolysis, **vol. 78**, 2007, pp. 291-300
[2] *C. Di Blasi*, "Comparison of semi-global mechanisms for primary pyrolysis of lignocellulosic fuels", J. Anal. Appl. Pyrolysis, **vol. 47**, 1998, pp. 43-64
[3] *C. Di Blasi*, "Modeling chemical and physical processes of wood and biomass pyrolysis", Prog. Energy Combust. Sci., **vol. 34**, 2008, pp. 47-90
[4] *M.F. Parihar, M. Kamil, H.B. Goyal, A.K. Gupta and A.K. Bhatnagar*, "An experimental study on pyrolysis of biomass", Trans IChemE, **vol. 85 (B5)**, 2007, pp. 458-465
[5] *Y. Richardson, J. Blin, G. Volle, J. Motuzas and A. Julbe*, "In situ generation of Ni metal nanoparticles as catalyst for H2-rich syngas production from biomass gasification", Applied Catalysis A: General, **vol. 382**, 2010, pp. 220-230
[6] *R. Zanzi*, Pyrolysis of biomass, Dissertation, Royal Institute of Technology, Stockholm, 2001
[7] *J.F. Gonzalez, J.M. Encinar, J.L. Canito, E. Sabio and M. Chacon*, "Pyrolysis of cherry stones: energy uses of the different fractions and kinetic study", J. Anal. Appl. Pyrolysis, **vol. 67**, 2003, pp. 165-190
[8] *S. Xiu, Z. Li, B. Li, W. Yi and X. Bai*, "Devolatilization characteristics of biomass at flash heating rate", Fuel, 85, 2006, pp. 664-670
[9] *C. Acikgoz, O. Onay and O.M. Kockar*, "Fast pyrolysis of linseed: product yields and compositions", J. Anal. Appl. Pyrolysis, **vol. 71**, 2004, pp. 417-429
[10] *A. Çağlar and A. Demirbaş*, "Hydrogen rich gas mixture from olive husk via pyrolysis", Energ. Convers. Manage., **vol. 43**, 2002a, pp. 109-117

[11] *A. Çağlar and A. Demirbaş*, "Conversion of cotton cocoon shell to hydrogen rich gaseous products by pyrolysis", Energ. Convers. Manage., **vol. 43**, 2002b, pp. 489-497
[12] *T. Damartzis, G. Ioannidis and A. Zabaniotou*, "Simulating the behavior of a wire mesh reactor for olive kernel fast pyrolysis", Chem. Eng. J., **vol. 136**, 2008, pp. 320-330
[13] *A. Demirbaş*, "Gaseous products from biomass by pyrolysis and gasification: effects of catalyst on hydrogen yield", Energ. Convers. Manage., **vol. 43**, 2002a, pp. 897-909
[14] *A. Demirbaş*, "Partly chemical analysis of liquid fraction of flash pyrolysis products from biomass in the presence of sodium carbonate", Energ. Convers. Manage., **vol. 43**, 2002b, pp. 1801-1809
[15] *A. Demirbaş*, "Effect of temperature on pyrolysis products from four nut shells", J. Anal. Appl. Pyrolysis, **vol. 76**, 2006, pp. 285-289
[16] *C. Di Blasi, G. Signorelli, C. Di Russo and G. Rea*, "Product distribution from pyrolysis of wood and agricultural residues", Ind. Eng. Chem. Res., **vol. 38**, 1999, pp. 2216-2224
[17] *A. Zabaniotou and O. Ioannidou*, "Evaluation of utilization of corn stalks for energy and carbon material production by using rapid pyrolysis at high temperature", Fuel, **vol. 87**, 2008, pp. 834-843
[18] *F. Yu, R. Ruan and P. Steele*, "Consecutive reaction model for the pyrolysis of corn cob", Trans. ASABE, **vol. 51**, 2008, pp. 1023-1028
[19] *M.C. Blanco Lopez, C.G., Blanco, A. Martinez Alonso and J.M.D. Tascon*, "Composition of gases released during olive stones pyrolysis", J. Anal. Appl. Pyrolysis, **vol. 65**, 2002, pp. 313-322
[20] *T. Dobre, O.C. Pârvulescu, G. Iavorschi, A. Stoica and M. Stroescu*, "Catalytic effects at pyrolysis of wheat grains impregnated with nickel salts", International Journal of Chemical Reactor Engineering, **vol. 8**, 2010a, pp. 1968-1992
[21] *T. Dobre, O.C. Pârvulescu, L. Ceatră, M. Stroescu and G. Iavorschi*, "Catalytic effects at the vegetal materials pyrolysis", in Proceedings of the 6th European Meeting on Chemical Industry and Environment (EMChIE), May 17-19, 2010b, Mechelen, Belgium, **vol. 1**, pp. 605-615
[22] *P.J. White and L.A. Johnson*, Corn: chemistry and technology. American Assoc. of Cereal Chemists, St. Paul, MN, USA, 2003
[23] *V. Singh and D. Johnston*, Advances in Food and Nutrition Research, **vol. 48**, Elsevier Academic Press, San Diego, USA, 2004
[24] *O.C. Pârvulescu, T. Dobre, L. Ceatră, G. Iavorschi and R. Mirea*, "Characteristics of corn grains pyrolysis in a fixed bed reactor", Revista de Chimie, **vol. 62**, 2011, pp. 89-94
[25] *F. Suárez-García, A. Martínez-Alonso and J.M.D. Tascón*, "Pyrolysis of apple pulp: effect of operation conditions and chemical additives", J. Anal. Appl. Pyrolysis, **vol. 62**, 2002, pp. 93-109
[26] *A. Aboulkas, K. El harfi, A. El bouadili, M. Nadifiyine, M. Benchanaa and A. Mokhlisse*, "Pyrolysis kinetics of olive residue/plastic mixtures by non-isothermal thermogravimetry", Fuel Process. Technol., **vol. 90**, 2009, pp. 722-728
[27] *L.S. Guinesi, A.L. da Roz, E. Corradini, L.H.C. Mattoso, E.M. Teixeira and A.A.S. Curvelo*, "Kinetics of thermal degradation applied to starches from different botanical origins by non-isothermal procedures", Thermochim. Acta, **vol. 447**, 2006, pp. 190-196
[28] *S. Hu, A. Jess and M. Xu*, "Kinetic study of Chinese biomass slow pyrolysis: Comparison of different kinetic models", Fuel, **vol. 86**, 2007, pp. 2778-2788
[29] *M. Jeguirim and G. Trouvé*, "Pyrolysis characteristics and kinetics of Arundo donax using thermogravimetric analysis", Biores. Technol., **vol. 100**, 2009, pp. 4026-4031
[30] *Z. Li, W. Zhao, B. Meng, C. Liu, Q. Zhu and G. Zhao*, "Kinetic study of corn straw pyrolysis: Comparison of two different three-pseudocomponent models", Biores. Technol., **vol. 99**, 2008, pp. 7616-7622

[31] *T. Dobre and J. Sanchez Marcano*, Chemical engineering - modelling, simulation and similitude, Wiley VCH, 2007
[32] *O. Ioannidou and A. Zabaniotou*, "Agricultural residues as precursors for activated carbon production: A review", Renew. Sustain. Energ. Rev., **vol. 11**, 2007, pp. 1966-2005